Explicit Analysis of RC Polyphase Filter for I, Q Signal Generation and Image Rejection

Jian KANG, Haruo KOBAYASHI, Takashi KITAHARA, Seiya TAKIGAMI, Hiroshi SADAMURA
Dept. of Electronic Engineering, Gunma University, 1-5-1 Tenjin-cho Kiryu 376-8515 Japan
phone: 81-277-30-1788 fax: 81-277-30-1707 e-mail: k_haruo@el.gunma-u.ac.jp

Abstract – RC polyphase filters are important components in analog front-ends of wireless transceivers. This paper derives explicit frequency transfer functions for first-, second- and third-order RC polyphase filters, allowing systematic exploitation of their characteristics.

Keywords: Polyphase Filter, RF Circuit, Image Rejection, Wireless Transceiver, Complex Signal

I. Introduction

RC polyphase filters are important components in analog front-ends of wireless transceivers; they are used for In-Phase and Quadrature (I and Q) signal generation and for image rejection [1, 2, 3, 4, 5]. However, to the best of our knowledge, up to now their design has been based on simulation [3]. In this paper we have derived their frequency transfer functions analytically, to allow their characteristics to be exploited systematically. We believe that the explicit derivation of the frequency transfer functions of second and third-order RC polyphase filters is new.

Since the RC polyphase filter is a circulant structure, circulant matrices are extensively used for its analysis [6, 7], and in this paper we denote a 4x4 circulant matrix as follows:

$$circl(a,b,c,d) := \begin{bmatrix} a & b & c & d \\ d & a & b & c \\ c & d & a & b \\ b & c & d & a \end{bmatrix}.$$

II. Roles of RC Polyphase Filters

This section reviews the usage of RC polyphase filters in analog front-ends of wireless transceiver systems.

Example 1:

In Fig.1(a), let $I_{in}(t) = \cos(\omega_{LO}t)$, and $Q_{in}(t) \equiv 0$. Then we have

$$I_{out}(t) = A_I \cos(\omega_{LO}t + \theta),$$
$$Q_{out}(t) = A_Q \sin(\omega_{LO}t + \theta),$$

and Fig.1(c) shows their SPICE simulation waveforms. (Here A_I, A_Q and θ are appropriate constants.) Thus the RC polyphase filter can be used for generating cosine and sine signals from a single sinusoidal signal (Fig.1(b)), and the cosine and sine signals are supplied to mixers used for up conversion or down conversion.

Example 2:

However, the RC polyphase filter in Fig.1(a) has component sensitivity problems. If $\omega_{LO} = 1/(R_1C_1)$ is satisfied then the amplitudes of $I_{out}(t)$ and $Q_{out}(t)$ are exactly the same ($A_I = A_Q$), but if $\omega_{LO} \neq 1/(R_1C_1)$, then A_I and A_Q can be very different. Cascading two RC polyphase filters as shown in Fig.2(a) alleviates of this problem. Fig.1(d) shows waveforms of $I_{out}(t)$, $Q_{out}(t)$ in Fig.1(a) while Fig.2(b) shows those in Fig.2(a) for $\omega_{LO} = 2/(R_1C_1)$. We see that the amplitudes of $Q_{out}(t)$, $I_{out}(t)$ in Fig.1(a) are very different but those in Fig.2(a) are quite similar even though in both cases the phase difference between $Q_{out}(t)$ and $I_{out}(t)$ are exactly $\pi/2$ [rad]. We note that cascading three RC polyphase filters can further reduce the amplitude difference.

Example 3:

Consider the case of two signal generators which produce cosine and sine signals respectively but with third-order harmonics. The RC polyphase filter can be used to cancel the third-order harmonics and generate pure cosine and sine signals (Fig.3(a)). In Fig.1(a), letting

$$I_{in}(t) = \cos(\omega_{LO}t) + a\cos^3(\omega_{LO}t)$$
$$= (1 + \frac{3a}{4})\cos(\omega_{LO}t) + \frac{a}{4}\cos(3\omega_{LO}t),$$

$$Q_{in}(t) = \sin(\omega_{LO}t) + a\sin^3(\omega_{LO}t)$$
$$= (1 + \frac{3a}{4})\sin(\omega_{LO}t) - \frac{a}{4}\sin(3\omega_{LO}t).$$

In other words,

$$I_{in}(t) + jQ_{in}(t) = (1 + \frac{3a}{4})e^{j\omega_{LO}t} + \frac{a}{4}e^{-j3\omega_{LO}t}$$

where a is a constant. If $3\omega_{LO} = 1/(R_1C_1)$, then we have the following:

$$I_{out}(t) = A\cos(\omega_{LO}t + \theta),$$
$$Q_{out}(t) = A\sin(\omega_{LO}t + \theta).$$

In other words,

$$I_{out}(t) + jQ_{out}(t) = Ae^{j(\omega_{LO}t+\theta)}$$

where A and θ are appropriate constants. We see that, for complex input signals, the RC polyphase filter passes the frequency component ω_{LO} but it rejects $-3\omega_{LO}$. Fig.3(b) shows SPICE simulation waveforms of $I_{in}(t)$ and $Q_{in}(t)$ while Fig.3 (c) shows those of $I_{out}(t)$ and $Q_{out}(t)$.

Example 4:

Letting $\omega_{in} = 1/(R_1C_1)$ and applying $I_{in}(t) = \cos(\omega_{in}t)$ and $Q_{in}(t) = \sin(\omega_{in}t)$ to the circuit in Fig.1(a), and we have $I_{in}(t) = (\sqrt{2}/2)\cos(\omega_{in}t - \pi/4)$ and $Q_{in}(t) = (\sqrt{2}/2)\sin(\omega_{in}t - \pi/4)$. On the other hand, if we apply $I_{in}(t) = \cos(-\omega_{in}t) = \cos(\omega_{in}t)$, $Q_{in}(t) = \sin(-\omega_{in}t) = -\sin(\omega_{in}t)$ to the circuit in Fig.1(a), we have $I_{out}(t) = Q_{out}(t) \equiv 0$. Hence the RC polyphase filter passes the frequency component ω_{in} but it rejects $-\omega_{in}$, and so it works as an image rejection filter.

III. First Order RC Polyphase Filter

Let us consider the first-order RC polyphase filter in Fig.1 (a) and define the following:

$$I_{in}(t) := I_{in+}(t) - I_{in-}(t),$$
$$Q_{in}(t) := Q_{in+}(t) - Q_{in-}(t),$$
$$I_{out}(t) := I_{out+}(t) - I_{out-}(t),$$
$$Q_{out}(t) := Q_{out+}(t) - Q_{out-}(t).$$

Now let us define complex signals $V_{in}(t)$ and $V_{out}(t)$ as follows [8]:

$$V_{in}(t) := I_{in}(t) + jQ_{in}(t),$$
$$V_{out}(t) := I_{out}(t) + jQ_{out}(t).$$

Letting $V_{in}(j\omega)$ be the Fourier transform of $V_{in}(t)$ and so on, we have the following relationships:

$$\mathbf{v_{out}} = M_1\mathbf{v_{in}}.$$

Here

$$\mathbf{v_{in}} := (I_{in+}(j\omega), Q_{in+}(j\omega), I_{in-}(j\omega), Q_{in-}(j\omega))^T,$$

$$\mathbf{v_{out}} := (I_{out+}(j\omega), Q_{out+}(j\omega), I_{out-}(j\omega), Q_{out-}(j\omega))^T,$$

$$M_1 := circl(F_1(j\omega), 0, 0, H_1(j\omega)), \tag{1}$$

$$F_1(j\omega) := \frac{1}{1 + j\omega R_1C_1}, \quad H_1(j\omega) := \frac{-j\omega R_1C_1}{1 + j\omega R_1C_1}.$$

Then we obtain

$$\begin{bmatrix} I_{out}(j\omega) \\ Q_{out}(j\omega) \end{bmatrix} = \begin{bmatrix} F_1(j\omega) & -H_1(j\omega) \\ H_1(j\omega) & F_1(j\omega) \end{bmatrix} \begin{bmatrix} I_{in}(j\omega) \\ Q_{in}(j\omega) \end{bmatrix}. \tag{2}$$

We define the frequency transfer function for complex input and output signals $V_{in}(j\omega)$ and $V_{out}(j\omega)$ as follows:

$$G_1(j\omega) := \frac{V_{out}(j\omega)}{V_{in}(j\omega)}.$$

Then we obtain

$$G_1(j\omega) = F_1(j\omega) + jH_1(j\omega) = \frac{1 + \omega R_1C_1}{1 + j\omega R_1C_1}. \tag{3}$$

Note that $|G_1(j\omega)| \neq |G_1(-j\omega)|$ in general (see Fig.4 (a)), and gain and phase are given by

$$|G_1(j\omega)| = \frac{|1 + \omega R_1C_1|}{\sqrt{1 + (\omega R_1C_1)^2}}$$

$$\tan\angle G_1(j\omega) = -\omega R_1C_1.$$

This frequency transfer function $G_1(j\omega)$ characterizes a first-order RC polyphase filter for complex signals.

Remark (i) Noting that $G(j\omega)$ has a zero at $\omega = -1/(R_1C_1)$, we have

$$\angle G_1(j\omega) = \begin{cases} -\angle G_1(-j\omega) & (0 \le \omega < \frac{1}{R_1C_1}) \\ \angle G_1(-j\omega) - \pi & (\frac{1}{R_1C_1} < \omega). \end{cases}$$

See Fig.4 (b) and Fig.5.

(ii) The frequency transfer function G_1 in eq.(3) can explain Example 1. Letting

$$V_{in}(t) = \cos(\omega_{LO}t) = \frac{1}{2}[e^{j\omega_{LO}t} + e^{-j\omega_{LO}t}],$$

and $\omega_{LO} = 1/(R_1C_1)$, then

$$V_{out}(t) = \frac{1}{2}[|G_1(j\omega_{LO})|e^{j(\omega_{LO}t+\angle G_1(j\omega_{LO}))}$$

$$+|G_1(-j\omega_{LO})|e^{j(\omega_{LO}t+\angle G_1(-j\omega_{LO}))}]$$

$$= \frac{\sqrt{2}}{2}e^{j(\omega_{LO}t-\pi/4)}$$

because

$$|G_1(j\omega)|_{\omega=-\frac{1}{R_1C_1}} = 0, \quad |G_1(j\omega)|_{\omega=\frac{1}{R_1C_1}} = \sqrt{2},$$

$$\tan \angle G_1(j\omega)|_{\omega=\frac{1}{R_1C_1}} = -1.$$

Similarly Examples 3 and 4 can be explained using $G_1(j\omega)$.
(iii) When

$$\begin{bmatrix} I_{out}(j\omega) \\ Q_{out}(j\omega) \end{bmatrix} = \begin{bmatrix} K(j\omega) & L(j\omega) \\ M(j\omega) & N(j\omega) \end{bmatrix} \begin{bmatrix} I_{in}(j\omega) \\ Q_{in}(j\omega) \end{bmatrix},$$

the condition for it to have the given frequency transfer function for complex signals (namely, the condition for it to be an Hilbert filter [3]) is

$$K(j\omega) = N(j\omega), \qquad L(j\omega) = -M(j\omega)$$

and eq.(2 satisfies this, which is because the matrix M_1 defined in eq.(1) is circulant [6, 7].
(iv) It is well-known that the frequency transfer function is a Fourier transform of the impulse response when input and output are real signals; here we consider the case that they are complex signals. Suppose that for $I_{in}(t) = \delta(t), Q_{in}(t) \equiv 0$,

$$I_{out}(t) = g_{ii}(t), \qquad Q_{out}(t) = g_{qi}(t)$$

and for $t < 0$, $g_{ii}(t) = g_{qi}(t) \equiv 0$. Then we have

$$G_1(j\omega) = \int_{-\infty}^{\infty} (g_{ii}(t) + jg_{qi}(t))e^{-j\omega t}dt$$

because

$$H_1(j\omega) = \int_{-\infty}^{\infty} g_{ii}(t)e^{-j\omega t}dt,$$

$$F_1(j\omega) = \int_{-\infty}^{\infty} g_{qi}(t)e^{-j\omega t}dt$$

and eq.(2) holds.
(v) Suppose that for $I_{in}(t) \equiv 0, Q_{in}(t) = \delta(t)$,

$$I_{out}(t) = g_{iq}(t) \qquad Q_{out}(t) = g_{qq}(t)$$

and for $t < 0$, $g_{iq}(t) = g_{qq}(t) \equiv 0$. Then it follows from eq.(2) that

$$g_{ii}(t) = g_{qq}(t), \qquad g_{iq}(t) = -g_{qi}(t).$$

IV. Second-Order RC Polyphase Filter

Fig.2 (a) shows a second-order RC polyphase filter, and we have derived its frequency transfer function $G_2(j\omega)$ explicitly using Mathematica:

$$G_2(j\omega) = \frac{(1+\omega R_1C_1)(1+\omega R_2C_2)}{1-\omega^2R_1C_1R_2C_2 + j\omega(C_1R_1 + C_2R_2 + 2R_1C_2)}. \tag{4}$$

See Appendix A for basic equations used to derive $G_2(j\omega)$. Fig.6 shows $|G_2(j\omega)|$ with respect to ω, and we see that $G_2(j\omega)$ has zeros at the angular frequencies $\omega = -1/(R_1C_1)$ and $-1/(R_2C_2)$. Also the same arguments as the first-order RC polyphase filter case hold.

V. Third-Order RC Polyphase Filter

Fig.7 shows a third-order RC polyphase filter, and again we have derived the frequency transfer function $G_3(j\omega)$ explicitly using Mathematica:

$$G_3(j\omega) := \frac{N_3(j\omega)}{D_3(j\omega)}. \tag{5}$$

Here

$$N_3(j\omega) := (1+\omega R_1C_1)(1+\omega R_2C_2)(1+\omega R_3C_3),$$

$$D_3(j\omega) := D_{3R}(\omega) + jD_{3I}(\omega),$$

$$D_{3R}(\omega) := 1 - \omega^2[R_1C_1R_2C_2 + R_2C_2R_3C_3 + R_1C_1R_3C_3 + 2R_1C_3(R_2C_2 + R_2C_1 + R_3C_2)],$$

$$D_{3I}(\omega) := \omega[R_1C_1 + R_2C_2 + R_3C_3 + 2(R_1C_2 + R_2C_3 + R_1C_3)] - \omega^3R_1C_1R_2C_2R_3C_3.$$

See Appendix B for basic equations used to derive $G_3(j\omega)$. Fig.8 shows $|G_3(j\omega)|$ with respect to ω, and we see that $G_3(j\omega)$ has zeros at the angular frequencies $\omega = -1/(R_1C_1)$, $-1/(R_2C_2)$ and $-1/(R_3C_3)$.

VI. Conclusions

We have derived explicit frequency transfer functions for first-, second- and third-order RC polyphase filters; those of higher-order filters could be obtained with the same approach. Also we have characterized RC polyphase filters using frequency transfer functions.

We would like to thank K. Wilkinson for valuable discussions.

References

[1] J. Crols and M. Steyeart, *CMOS Wireless Transceiver Design,* Kluwer Academic Publishers (1997).

[2] S. Sheng and R. Broderson, *Low Power Wireless Communication Applications - A Wideband CDMA System Design - ,* Kluwer Academic Publishers (1998).

[3] F. Behbahani, Y. Kishigami, J. Leete and A. A. Abidi, "CMOS Mixers and Polyphase Filters for Large Image Rejection," *IEEE J. Solid-State Circuits,* vol.36, no.6, pp.873-887 (June 2001).

[4] A. Rofougaran, G. Chang, J. J. Rael, J. Y.-C. Chang, M. Rofougaran, P. J. Chang, M. Djafari, M.-K.Ku, E. R. Roth, A. A. Abidi and H. Samueli, "A Single-Chip 9–MHz Spread-Spectrum Wireless Transceiver in 1-μm CMOS - Part I; Architecture and Transmitter Design," *IEEE J. Solid-State Circuits,* vol.33, no.4, pp.515-534 (April 1998).

[5] M. Steyeart, M. Borremans, J. Janssens, B. D. Muer, N. Itoh, J. Carnicky, J. Crols, E. Morifuji, H. S. Momose and W. Sansen, "A Single-Chip CMOS Transceiver for DCS-1800 Wireless Communications," *ISSCC Digest of Technical Papers,* vol.41, pp.48-49 (Feb. 1998).

[6] P. J. Davis, *Circulant Matrices,* New York: Wiley (1979).

[7] H. Kobayashi, T. Matsumoto, and J. Sanekata, "Two-Dimensional Spatio-Temporal Dynamics of Analog Image Processing Neural Networks," *IEEE Trans. on Neural Networks,* vol.6, no.5, pp.1148-1164 (1995).

[8] L. Cohen, *Time-Frequency Analysis,* Prentice Hall (1995).

Appendix A

This appendix gives basic equations used to derive $G_2(j\omega)$ in eq.(4). According to Kirchhoff's Current Law in Fig.2 (a), we have

$$A_1\mathbf{v_{in}} + B_1\mathbf{v_{out}} = y_1\mathbf{v_m}$$

$$(1/R_2 + j\omega C_2)\mathbf{v_{out}} = A_2\mathbf{v_m}.$$

Here

$$\begin{aligned}
&\mathbf{v_{in}} := (I_{in+}, Q_{in+}, I_{in-}, Q_{in-})^T,\\
&\mathbf{v_{out}} := (I_{out+}, Q_{out+}, I_{out-}, Q_{out-})^T,\\
&\mathbf{v_m} := (v_a, v_b, v_c, v_d)^T,\\
&A_1 := circl(1/R_1, 0, 0, j\omega C_1),\\
&B_1 := circl(1/R_1, j\omega C_1, 0, 0),\\
&A_2 := circl(1/R_2, 0, 0, j\omega C_2),\\
&y_1 := 1/R_1 + 1/R_2 + j\omega(C_1 + C_2).
\end{aligned}$$

Then we obtain $\mathbf{v_{out}} = M_2\mathbf{v_{in}}$. Here $M_2 := circl(a_2, b_2, c_2, d_2)$ and a_2, b_2, c_2, d_2 are defined appropriately. Then after manipulation of the above expressions, we have

$$\begin{bmatrix} I_{out}(j\omega) \\ Q_{out}(j\omega) \end{bmatrix} = \begin{bmatrix} F_2(j\omega) & -H_2(j\omega) \\ H_2(j\omega) & F_2(j\omega) \end{bmatrix} \begin{bmatrix} I_{in}(j\omega) \\ Q_{in}(j\omega) \end{bmatrix}$$

$$F_2(j\omega) = a_2 - c_2, \qquad H_2(j\omega) = b_2 - d_2,$$

$$G_2(j\omega) = F_2(j\omega) + jH_2(j\omega)$$

which yields to the final form of $G_2(j\omega)$ in eq.(4).

Appendix B

This appendix gives basic equations used to derive $G_3(j\omega)$ in eq.(5). According to Kirchhoff's Current Law in Fig.7, we have

$$\begin{aligned}
&A_1\mathbf{v_{in}} + B_2\mathbf{v_{m2}} = y_1\mathbf{v_{m1}}\\
&A_2\mathbf{v_{m1}} + B_3\mathbf{v_{out}} = y_2\mathbf{v_{m2}}\\
&(1/R_3 + j\omega C_3)\mathbf{v_{out}} = A_3\mathbf{v_{m2}}.
\end{aligned}$$

Here

$$\begin{aligned}
&\mathbf{v_{in}} := (I_{in+}, Q_{in+}, I_{in-}, Q_{in-})^T\\
&\mathbf{v_{out}} := (I_{out+}, Q_{out+}, I_{out-}, Q_{out-})^T\\
&\mathbf{v_{m1}} := (v_a, v_b, v_c, v_d)^T\\
&\mathbf{v_{m2}} := (v_e, v_f, v_g, v_h)^T\\
&A_1 := circl(1/R_1, 0, 0, j\omega C_1)\\
&A_2 := circl(1/R_2, 0, 0, j\omega C_2)\\
&A_3 := circl(1/R_3, 0, 0, j\omega C_3)\\
&B_2 := circl(1/R_2, j\omega C_2, 0, 0)\\
&B_3 := circl(1/R_3, j\omega C_3, 0, 0)\\
&y_1 := 1/R_1 + 1/R_2 + j\omega(C_1 + C_2)\\
&y_2 := 1/R_2 + 1/R_3 + j\omega(C_2 + C_3).
\end{aligned}$$

Then we obtain $\mathbf{v_{out}} = M_3\mathbf{v_{in}}$. Here $M_3 := circl(a_3, b_3, c_3, d_3)$ and a_3, b_3, c_3, d_3 are defined appropriately. Then after manipulation of the above expressions, we have

$$\begin{bmatrix} I_{out}(j\omega) \\ Q_{out}(j\omega) \end{bmatrix} = \begin{bmatrix} F_3(j\omega) & -H_3(j\omega) \\ H_3(j\omega) & F_3(j\omega) \end{bmatrix} \begin{bmatrix} I_{in}(j\omega) \\ Q_{in}(j\omega) \end{bmatrix}$$

$$\begin{aligned}
F_3(j\omega) = a_3 - c_3, \qquad H_3(j\omega) = b_3 - d_3,\\
G_3(j\omega) = F_3(j\omega) + jH_3(j\omega),
\end{aligned}$$

which yields to the final form of $G_3(j\omega)$ in eq.(5).

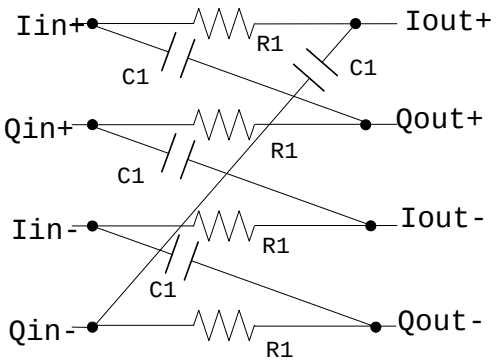

Fig.1 (a): The first-order RC polyphase filter.

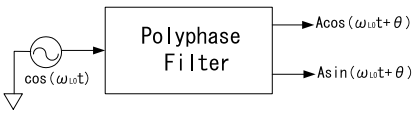

Fig.1 (b): Cosine and sine signal generation from a single sinusoidal signal.

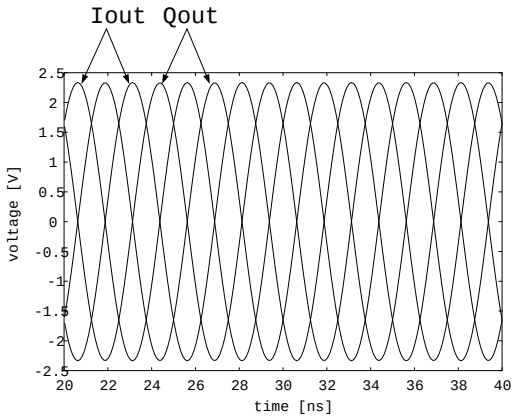

Fig.1 (c): SPICE simulation waveforms of $I_{out}(t)$ and $Q_{out}(t)$ when $R = 0.1592k\Omega, C = 5pF$ and $\omega_{LO}/(2\pi) = 1/(2\pi R_1 C_1) = 200MHz$.

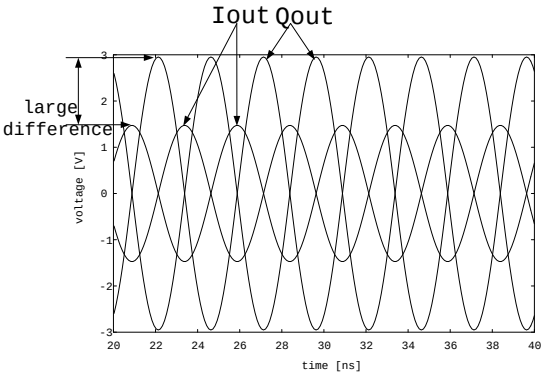

Fig.1 (d): SPICE simulation waveforms of $I_{out}(t)$ and $Q_{out}(t)$ when $R = 0.1592k\Omega, C = 10pF$ and $\omega_{LO}/(2\pi) = 2/(2\pi R_1 C_1) = 200MHz$.

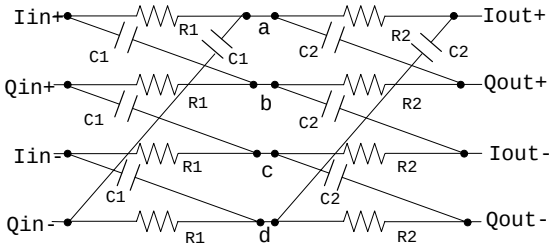

Fig.2 (a): The second-order RC polyphase filter.

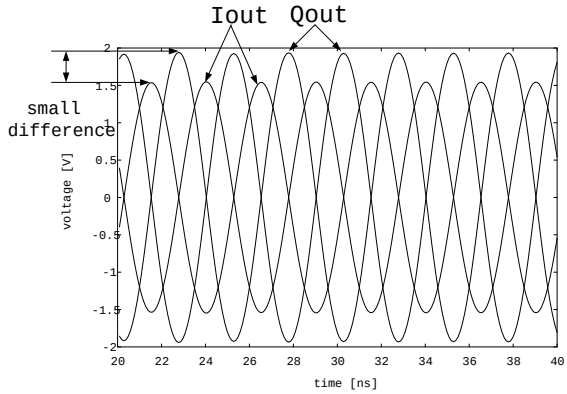

Fig.2 (b): SPICE simulation waveforms of $I_{out}(t)$ and $Q_{out}(t)$ when $R_1 = R_2 = 0.1592k\Omega, C_1 = C_2 = 10pF$ and $\omega_{LO}/(2\pi) = 2/(2\pi R_1 C_1) = 200MHz$.

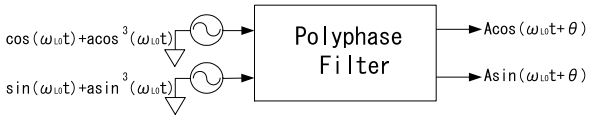

Fig.3 (a): Cosine and sine signal generation from two signals which include third-order harmonics.

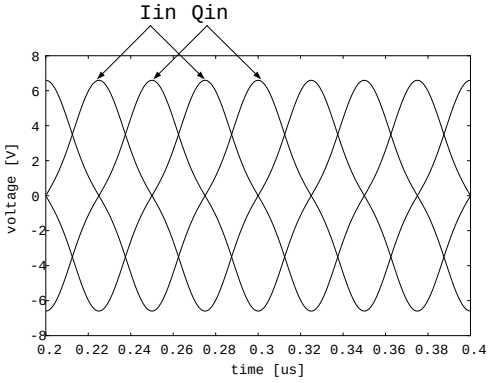

Fig.3 (b): SPICE simulation waveforms of $I_{in}(t)$ and $Q_{in}(t)$ when $R_1 = 530.516\Omega, C_1 = 1pF$ and $\omega_{LO}/(2\pi) = 1/(2\pi R_1 C_1) = 300MHz$.

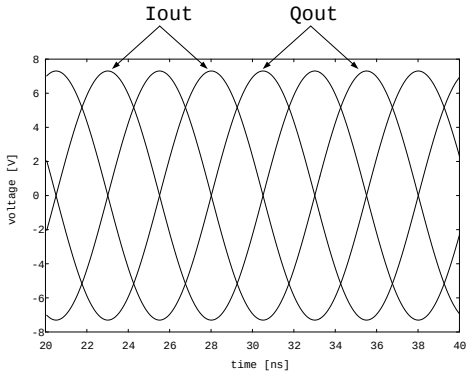

Fig.3 (c): SPICE simulation waveforms of $I_{out}(t)$ and $Q_{out}(t)$ when $R_1 = 530.516\Omega, C_1 = 1pF$ and $\omega_{LO}/(2\pi) = 1/(2\pi R_1 C_1) = 300MHz$.

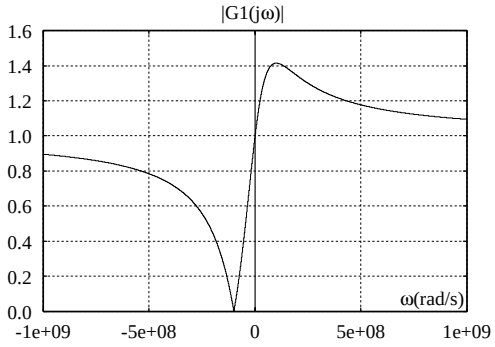

(a) Gain characteristics.

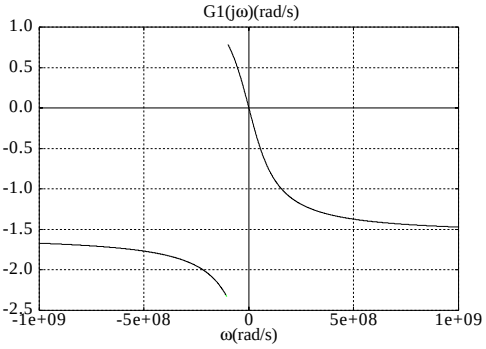

(b) Phase characteristics.

Fig.4 : Gain and phase characteristics of the first-order RC polyphase filter of Fig.1 (a) when $R_1 = 1k\Omega, C_1 = 10pF$.

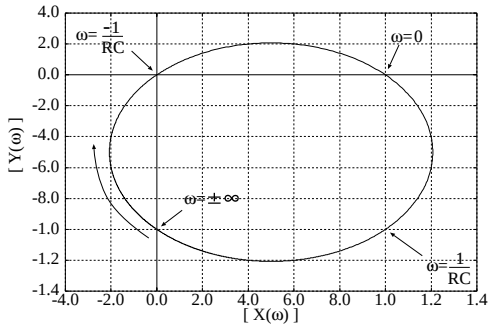

Fig.5 : Nyquist chart of the first-order RC polyphase filter transfer function $G_1(\jmath\omega)$ of Fig.1 (a), where $G_1(\jmath\omega) = X(\omega) + jY(\omega)$.

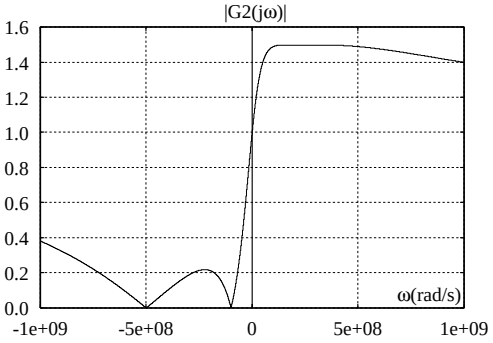

Fig.6 : Gain characteristics of the second-order RC polyphase filter of Fig.2 (a) when $R_1 = 1k\Omega, C_1 = 10pF, R_2 = 2k\Omega$ and $C_2 = 1pF$.

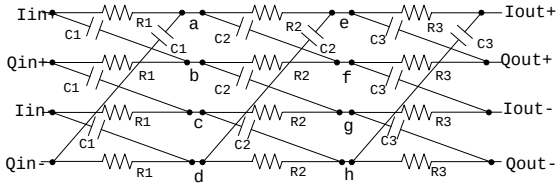

Fig.7 : The third-order RC polyphase filter.

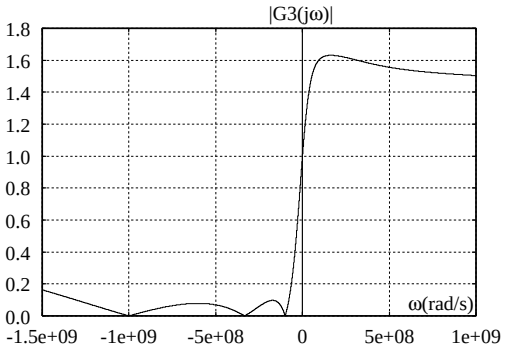

Fig.8: Gain characteristics of the third-order RC polyphase filter of Fig.7 when $R_1 = 1k\Omega, C_1 = 10pF$, $R_2 = 3k\Omega, C_2 = 1pF$, $R_3 = 5k\Omega$ and $C_3 = 0.2pF$.